Research Square

Preprints are preliminary reports that have not undergone peer review.
They should not be considered conclusive, used to inform clinical practice,
or referenced by the media as validated information.

Dexamethasone does not provide functional or biochemical neuroprotection in young rats with kaolin-induced hydrocephalus

Larissa Caires Giglio
Universidade de São Paulo
Otávio da Cunha Ferreira Neto
Universidade de São Paulo
Matheus Nagai Ribeiro do Val
Universidade de São Paulo
Felipe Issa Chodraui
Universidade de São Paulo
Hélio Rubens Machado
Universidade de São Paulo
Luiza da Silva Lopes
Universidade de São Paulo
Marcelo Volpon Santos
marcelovolpon@fmrp.usp.br
Universidade de São Paulo

Research Article

Keywords: Astrogliosis, glucocorticoids, hydrocephalus, neuroprotection

Posted Date: November 19th, 2026

DOI: https://doi.org/10.21203/rs.3.rs-11587242/v1

License: This work is licensed under a Creative Commons Attribution 4.0 International License.
Read Full License

Additional Declarations: No competing interests reported.

Abstract

Purpose

Glucocorticoids have anti-inflammatory properties that could provide neuroprotection and delay the need for cerebrospinal fluid diversion in hydrocephalus. We tested whether dexamethasone is neuroprotective in experimental hydrocephalus in young rats.

Methods

In a 2 × 2 design, male Wistar pups received intracisternal kaolin or no intervention on postnatal day 7 and daily intraperitoneal dexamethasone (0.5 mg/kg) or no treatment for 21 days. Groups: untreated controls (n = 11), dexamethasone-treated controls (n = 10), untreated hydrocephalic (n = 6) and treated hydrocephalic rats (n = 9). Body weight, ultrasonography (days 6 and 13), Morris water maze, glial fibrillary acidic protein (GFAP) immunohistochemistry, and GFAP and myelin basic protein (MBP) ELISA were analysed.

Results

Dexamethasone reduced weight gain (day 21: 42.3 ± 10.3 vs. 83.8 ± 12.3 g in treated vs. untreated hydrocephalic rats; 68.0 ± 11.3 vs. 94.0 ± 15.3 g in controls; $p < 0.001$). No treated kaolin-injected animal died (0/15 vs. 5/13; $p = 0.013$). Ventricular ratios did not differ between hydrocephalic groups. Dexamethasone prolonged escape latencies ($p = 0.003$); untreated hydrocephalic rats did not differ from controls, and probe-trial performance was similar. Hippocampal GFAP was 17-fold higher in untreated hydrocephalic rats than in controls and was not reduced by dexamethasone; callosal GFAP immunostaining appeared attenuated. Cortical MBP was about 50% lower in treated than untreated hydrocephalic rats, but this difference was not significant when one outlying value was included.

Conclusion

Dexamethasone caused substantial growth restriction in hydrocephalic rats but did not improve imaging, behavioural or biochemical outcomes.

Introduction

Hydrocephalus results from an imbalance between production, circulation and absorption of cerebrospinal fluid (CSF), leading to ventricular enlargement and, frequently, raised intracranial pressure [1, 28]. In children it may be congenital or acquired after hemorrhage, infection or tumours, and it remains a major cause of neurosurgical morbidity in infancy [19]. Congenital hydrocephalus affects

about 0.5–0.8 per 1,000 births [14, 17], and in a series of 150 shunted patients from our institution 47% were between 28 days and 6 months of age [18].

Shunting and endoscopic third ventriculostomy control ventricular distension but do not directly address secondary tissue injury, and shunt failure remains frequent [19]. Periventricular distension causes axonal injury, demyelination, reduced cerebral blood flow and reactive gliosis [7, 8]; in neonatal rats with kaolin-induced hydrocephalus, astrocytosis and microgliosis develop in the periventricular white matter [9, 21], and choroid plexus inflammation can drive CSF hypersecretion [20]. Pharmacological adjuncts that could mitigate such injury, particularly when surgery must be delayed, would certainly be helpful[6]; and anti-inflammatory drugs such as infliximab [22], minocycline [26, 31], edaravone [13] and celecoxib [10] have reduced gliosis in experimental models.

Glucocorticoids are potent regulators of inflammation [4, 12], frequently used as adjuncts in central nervous system infections [2, 15], and have been shown to reduce aberrant CSF formation and flow in animals [25, 30]. However, in newborn rats with post-hemorrhagic hydrocephalus, dexamethasone reduced gliosis without preventing ventricular dilatation [24], and postnatal dexamethasone has adverse neurodevelopmental effects in preterm infants and neonatal rodents [3, 11, 16, 32]. Therefore, we aimed to investigate whether dexamethasone confers neuroprotection in an experimental model of obstructive hydrocephalus, using a factorial design that also estimates its effects in non-hydrocephalic animals.

Methods

Ethics and animals

All procedures followed the guidelines of the Brazilian College of Animal Experimentation (COBEA) and were approved by the Ethics Committee on Animal Use of Ribeirão Preto Medical School, University of São Paulo (CEUA-FMRP-USP). Reporting follows the ARRIVE 2.0 guidelines [27]. Only male pups were used.

Design and allocation

The study followed a 2 × 2 factorial design (kaolin injection × dexamethasone). On postnatal day (PND) 7, pups were randomly allocated to control (C), dexamethasone-treated control (CTD), untreated hydrocephalic (HNT) or dexamethasone-treated hydrocephalic (HTD) groups. The day of kaolin injection was defined as experimental day 0 (D0) (Fig. 1a). Of 51 allocated animals, two C animals died before D21 of undetermined causes; of 13 HNT animals, five died during follow-up and two did not develop ventriculomegaly; of 15 HTD animals, none died and six did not develop ventriculomegaly. Kaolin-injected animals without ventriculomegaly on ultrasonography were excluded, so final groups had the following number of animals: C, n = 11; CTD, n = 10; HNT, n = 6; HTD, n = 9 (Fig. 1b).

Induction of hydrocephalus and treatment

On D0, HNT and HTD animals were anaesthetized with inhalatory isoflurane, and 0.04 mL of a sterile 15% kaolin suspension (Merck) in distilled water was injected slowly into the cisterna magna by percutaneous suboccipital puncture with a short-bevel dental needle (Mise 0.3); volume and concentration had been established in a previousstudy by our group. CTD and HTD animals received dexamethasone disodium phosphate (Decadron 2 mg/mL, Aché, Brazil; diluted to 0.1 mg/mL in 0.9% saline) at 0.5 mg/kg intraperitoneally once daily from D1 to D21 (PND 8–28), with doses calculated individually after daily weighing. All animals were weighed daily from D0 to D21.

Transcranial ultrasonography

Kaolin-injected animals were examined on D6 and D13 under isoflurane anaesthesia with a VEVO 2100 system (FUJIFILM VisualSonics, Toronto, Canada) and a 30-MHz transducer, using a method validated by our group [5]. Ventricular size was assessed on sagittal and coronal images and expressed as a ventricular ratio. On D6, ventricular borders could not be identified in three animals (one HTD, two HNT).

Morris water maze

A modified Morris water maze [29] was used: a circular pool divided into four quadrants, with a transparent platform 2 cm below the surface, in a dark room with a single wall-mounted light as spatial cue. On D9 (habituation), rats swam for 60 s without the platform, were placed on the platform for 15 s and performed four training trials from different cardinal points. On D10 and D11, rats performed two sessions per day (morning and afternoon, ≥ 4 h apart; M1, T1, M2, T2), each consisting of 15 s on the platform followed by four trials from the four cardinal points with a 60-s cut-off; the mean escape latency of the four trials was analysed. On D12, the platform was removed and crossings of the former platform quadrant were counted (probe trial).

Tissue collection, immunohistochemistry and ELISA

On D21 (PND 28), animals were deeply anaesthetised with intraperitoneal ketamine (100 mg/kg) and xylazine (10 mg/kg) and transcardiac perfusion with saline was undertaken. Their brains were divided in the midline. From the left hemisphere, the dorsal cortex overlying the lateral ventricle and the hippocampus were dissected, snap-frozen and stored at − 80°C. The right hemisphere was divided coronally at the optic chiasm and fixed in 3% paraformaldehyde in 0.1 M phosphate buffer at 4°C for 8 days.

Paraffin-embedded coronal sections (5 µm) were treated with 3% hydrogen peroxide, blocked with 10% goat serum and incubated overnight at 4°C with rabbit anti-GFAP (Z0334, Dako), followed by biotinylated goat anti-rabbit IgG (sc-2040, Santa Cruz Biotechnology; 1:2,000), streptavidin–HRP (405210, BioLegend; 1:400) and diaminobenzidine, with haematoxylin counterstaining. The corpus callosum was

photographed with a 40× objective (Nikon Eclipse E200; Moticam 10) and astroglial reactivity was assessed qualitatively.

The cortex and hippocampus were homogenized in PBS (1.5 mL and 400 µL, respectively) and centrifuged at 10,000 × g for 5 min at 4°C; total protein was measured by the Bradford method. GFAP and MBP were quantified by sandwich ELISA: plates were coated with polyclonal anti-GFAP (Z0334, Dako) or anti-MBP (ab28541, Abcam) at 1 µg/mL, blocked with 1% BSA, and incubated with standards (GFAP AG230, 1–150 ng/mL; MBP 13–104, 10–600 ng/mL; Merck Millipore) and samples in duplicate, monoclonal detection antibodies (anti-GFAP MAB360 and anti-MBP MAB386, Merck Millipore; 1:5,000), alkaline phosphatase-conjugated secondary antibody (ab6790, Abcam; 0.5 µg/mL) and p-nitrophenyl phosphate substrate (Thermo Fisher Scientific). Absorbance was read at 405 nm (VersaMax, Molecular Devices), concentrations were interpolated from four-parameter logistic curves and normalised to total protein (ng/mL per µg protein).

Statistical analysis

Data were reported as mean ± standard deviation (SD) or median ± interquartile range(IQR). Outcomes were analysed by two-way analysis of variance (ANOVA) with hydrocephalus and dexamethasone as factors, followed by four pre-defined Welch contrasts with Holm adjustment (HNT vs. C, CTD vs. C, HTD vs. HNT, HTD vs. CTD); effect sizes are given with 95% confidence intervals (CI). Weight trajectories were analysed with a linear mixed model (random intercept and slope per animal) and log-transformed escape latencies with a linear mixed model (session × hydrocephalus × dexamethasone; random intercept per animal). Ultrasonographic ratios were compared with Mann–Whitney and Wilcoxon tests and proportions with Fisher's exact test. ELISA data were $\log_{10}$-transformed and reported as ratios of geometric means; values beyond three interquartile ranges from the group quartiles on the log scale were excluded from the primary analysis, and all analyses were repeated with all values. Analyses were performed in Python (SciPy, statsmodels); the analysis code was drafted with the assistance of a large language model (Claude, Anthropic) and checked by the authors. Two-sided $p < 0.05$ was considered significant.

Results

Survival and body weight

No dexamethasone-treated kaolin-injected animal died (0/15), compared with 5/13 untreated animals ($p = 0.013$) (Fig. 1b). Failure to develop ventriculomegaly occurred in 6/15 treated and 2/8 untreated survivors ($p = 0.66$). Initial weights were similar across groups (Table 1). Dexamethasone markedly impaired growth (Fig. 2): on D21, weights were 94.0 ± 15.3 g (C), 68.0 ± 11.3 g (CTD), 83.8 ± 12.3 g (HNT) and 42.3 ± 10.3 g (HTD) (dexamethasone effect $p < 0.001$; hydrocephalus effect $p < 0.001$; interaction $p = 0.083$). Dexamethasone reduced D21 weight by 26.0 g in controls (95% CI 13.8–38.2) and by 41.5 g in hydrocephalic animals (95% CI 27.8–55.2; both adjusted $p < 0.001$), whereas HNT did not differ from C

(− 10.2 g; 95% CI − 25.1 to 4.6; p = 0.16). Dexamethasone reduced the growth rate by 1.16 g/day (95% CI 0.69–1.63; p < 0.001).

Table 1
Descriptive results by group (mean ± SD unless stated) and two-way ANOVA p-values

Outcome	C	CTD	HNT	HTD	Two-way ANOVA p
n analysed	11	10	6	9	
Body weight D0 (g)	20.1 ± 2.5	19.6 ± 4.1	19.5 ± 3.1	19.1 ± 2.1	HC 0.604; DEX 0.624; HC×DEX 0.963
Body weight D21 (g)	94.0 ± 15.3	68.0 ± 11.3	83.8 ± 12.3	42.3 ± 10.3	HC < 0.001; DEX < 0.001; HC×DEX 0.083
Weight gain D0–D21 (g)	73.9 ± 15.3	48.5 ± 10.0	64.2 ± 12.3	23.2 ± 9.5	HC < 0.001; DEX < 0.001; HC×DEX 0.070
MWM latency M1 (s)	14.7 ± 7.9	25.0 ± 20.3	19.3 ± 18.0	33.5 ± 13.9	see mixed model†
MWM latency T1 (s)	9.0 ± 4.1	14.8 ± 8.7	11.9 ± 6.6	27.4 ± 13.9	
MWM latency M2 (s)	7.8 ± 4.1	13.1 ± 8.2	7.3 ± 3.3	19.9 ± 10.5	
MWM latency T2 (s)	8.7 ± 4.6	8.9 ± 4.1	11.7 ± 9.3	13.6 ± 9.6	
Probe: quadrant crossings	7.0 ± 1.3	7.2 ± 1.4	7.2 ± 2.3	5.6 ± 2.7	HC 0.223; DEX 0.420; HC×DEX 0.186
US ventricular ratio D13	—	—	0.40 ± 0.06	0.38 ± 0.09	MW p = 0.516
GFAP cortex‡	2.66 (2.41–3.21) [10]	2.94 (2.18–3.29) [9]	3.49 (2.02–5.38) [6]	5.94 (3.75–8.28) [9]	HC 0.008; DEX 0.128; HC×DEX 0.063
GFAP hippocampus‡	4.23 (3.00–8.53) [11]	3.96 (2.86–10.09) [10]	83.07 (47.56–103.73) [6]	45.80 (9.11–174.44) [9]	HC < 0.001; DEX 0.845; HC×DEX 0.698

C, control; CTD, dexamethasone-treated control; HNT, untreated hydrocephalic; HTD, dexamethasone-treated hydrocephalic; HC, hydrocephalus factor; DEX, dexamethasone factor; MWM, Morris water maze; US, ultrasonography; MW, Mann–Whitney.

† Linear mixed model on $\log_{10}$ latency: session p < 0.001; DEX p = 0.003; HC p = 0.109; HC×DEX p = 0.232; session×DEX p = 0.048.

‡ ELISA values in ng/mL per µg total protein, median (IQR) [n]; ANOVA on $\log_{10}$ values after exclusion of extreme values (Tukey far-out rule); see text for sensitivity analyses.

Outcome	C	CTD	HNT	HTD	Two-way ANOVA p
MBP cortex‡	3.44 (2.59–5.25) [11]	2.79 (2.24–6.46) [10]	3.58 (3.05–3.79) [6]	1.85 (1.60–2.67) [8]	HC 0.042; DEX 0.082; HC×DEX 0.157
MBP hippocampus‡	4.01 (2.84–4.60) [7]	3.52 (2.80–8.64) [7]	4.34 (3.85–5.31) [5]	4.68 (3.81–5.70) [6]	HC 0.313; DEX 0.766; HC×DEX 0.936

C, control; CTD, dexamethasone-treated control; HNT, untreated hydrocephalic; HTD, dexamethasone-treated hydrocephalic; HC, hydrocephalus factor; DEX, dexamethasone factor; MWM, Morris water maze; US, ultrasonography; MW, Mann–Whitney.

† Linear mixed model on $\log_{10}$ latency: session $p < 0.001$; DEX $p = 0.003$; HC $p = 0.109$; HC×DEX $p = 0.232$; session×DEX $p = 0.048$.

‡ ELISA values in ng/mL per µg total protein, median (IQR) [n]; ANOVA on $\log_{10}$ values after exclusion of extreme values (Tukey far-out rule); see text for sensitivity analyses.

Ventricular size

Ventricular ratios on D13 did not differ between HNT (0.40 ± 0.06) and HTD (0.38 ± 0.09; $p = 0.52$) (Fig. 3). Between D6 and D13 the ratio increased in 3 of 4 HNT animals with paired examinations and decreased in 1, whereas in HTD it increased in 3 of 8, decreased in 4 and was unchanged in 1; the change did not differ between groups ($p = 0.39$).

Morris water maze

Latencies decreased across sessions in all groups ($p < 0.001$; Fig. 4a). Dexamethasone prolonged latencies (main effect $p = 0.003$), an effect that diminished over sessions (session × dexamethasone $p = 0.048$); there was no effect of hydrocephalus ($p = 0.11$) and no interaction ($p = 0.23$). HNT did not differ from C in any session. HTD latencies exceeded HNT latencies on T1 (27.4 ± 13.9 vs. 11.9 ± 6.6 s; adjusted $p = 0.054$) and M2 (19.9 ± 10.5 vs. 7.3 ± 3.3 s; adjusted $p = 0.029$), but not on T2 (13.6 ± 9.6 vs. 11.7 ± 9.3 s; $p = 0.70$). The larger reduction from M1 to T2 in HTD reflected its longer initial latency (33.5 ± 13.9 s). Probe-trial crossings did not differ (C 7.0 ± 1.3; CTD 7.2 ± 1.4; HNT 7.2 ± 2.3; HTD 5.6 ± 2.7; $p = 0.44$; Fig. 4b).

GFAP and MBP

GFAP immunostaining in the corpus callosum was faint in controls, with thin astrocytic processes, and intense in untreated hydrocephalic animals, whose corpus callosum was visibly thinned. In treated hydrocephalic animals, reactive astrocytes were present, but staining appeared less intense (Fig. 5); this was not quantified.

Hippocampal GFAP was markedly higher in hydrocephalic animals ($p < 0.001$), 16.8-fold higher in HNT than in C (95% CI 4.9–57.6; adjusted $p = 0.003$) and was not reduced by dexamethasone (HTD vs. HNT ratio 0.73; 95% CI 0.09–5.61; Fig. 6b; Table 2). One HTD sample had a value more than 20-fold above the next highest; rank-based results were unchanged. Cortical GFAP showed a hydrocephalus effect ($p = 0.008$), with no difference between HNT and C (ratio 1.15; 95% CI 0.60–2.22) or between HTD and HNT (ratio 2.05; 95% CI 0.89–4.73) (Fig. 6a).

Table 2
Pre-defined pairwise contrasts (effect estimate with 95% CI; Holm-adjusted Welch p-value)

Outcome	HNT vs C (hydrocephalus)	CTD vs C (DEX, controls)	HTD vs HNT (DEX, hydrocephalus)	HTD vs CTD
Body weight D21 (g)	-10.2 (− 25.1 to 4.6); p = 0.158	-26.0 (− 38.2 to − 13.8); p < 0.001	-41.5 (− 55.2 to − 27.8); p < 0.001	-25.7 (− 36.2 to − 15.3); p < 0.001
MWM mean latency, 4 sessions (s)	2.5 (− 5.5 to 10.4); p = 0.475	5.4 (− 1.2 to 12.0); p = 0.198	11.0 (1.7 to 20.4); p = 0.098	8.1 (− 0.6 to 16.8); p = 0.196
MWM latency T2 (s)	2.9 (− 6.8 to 12.7); p = 1.000	0.2 (− 3.8 to 4.2); p = 1.000	1.9 (− 9.0 to 12.9); p = 1.000	4.7 (− 3.0 to 12.3); p = 0.814
Probe crossings	0.2 (− 2.3 to 2.6); p = 1.000	0.2 (− 1.1 to 1.5); p = 1.000	-1.6 (− 4.5 to 1.3); p = 0.732	-1.6 (− 3.9 to 0.6); p = 0.529
GFAP cortex	×1.15 (0.60–2.22); p = 1.000	×0.98 (0.77–1.24); p = 1.000	×2.05 (0.89–4.73); p = 0.259	×2.42 (1.22–4.78); p = 0.066
GFAP hippocampus	×16.82 (4.92–57.56); p = 0.003	×1.06 (0.54–2.11); p = 1.000	×0.73 (0.09–5.61); p = 1.000	×11.47 (1.72–76.74); p = 0.052
MBP cortex (primary)	×0.89 (0.55–1.46); p = 1.000	×0.89 (0.49–1.60); p = 1.000	×0.50 (0.31–0.79); p = 0.026	×0.50 (0.29–0.89); p = 0.061
MBP cortex (all values)	×0.89 (0.55–1.46); p = 1.000	×0.89 (0.49–1.60); p = 1.000	×0.68 (0.30–1.55); p = 1.000	×0.69 (0.29–1.64); p = 1.000
MBP hippocampus	×1.34 (0.89–2.03); p = 0.576	×1.10 (0.39–3.09); p = 1.000	×1.06 (0.72–1.54); p = 1.000	×1.29 (0.46–3.59); p = 1.000

Outcome	HNT vs C (hydrocephalus)	CTD vs C (DEX, controls)	HTD vs HNT (DEX, hydrocephalus)	HTD vs CTD
Differences in means (95% CI) for weight and behaviour; ×, ratio of geometric means (95% CI) for ELISA (log_{10} scale). p, Holm-adjusted Welch t-test across the four contrasts within each outcome. Primary ELISA analyses exclude extreme values (cortex GFAP: two control values; cortex MBP: one HTD value; hippocampal MBP: one HNT value).				
Study design. **a** Experimental timeline; experimental day 0 (D0) corresponds to postnatal day (PND) 7. US, transcranial ultrasonography; MWM, Morris water maze; IHC, immunohistochemistry. **b** Flow of animals through the study. C, control; CTD, dexamethasone-treated control; HNT, untreated hydrocephalic; HTD, dexamethasone-treated hydrocephalic				
Body weight. **a** Daily body weight from D0 to D21 (mean ± SD, shaded). **b** Body weight on D21 in individual animals (bars, median and interquartile range); p-values are Holm-adjusted Welch contrasts. Filled symbols, untreated; open symbols, dexamethasone				
Ventricular ratio on transcranial ultrasonography on D6 and D13 in untreated (HNT) and dexamethasone-treated (HTD) hydrocephalic rats. Lines join measurements from the same animal; triangles indicate animals whose ventricular borders could not be identified on D6				
Morris water maze. **a** Escape latency in the four acquisition sessions (mean ± SEM); M1/T1, morning/afternoon of D10; M2/T2, morning/afternoon of D11. **b** Crossings of the former platform quadrant in the probe trial on D12 (individual animals; bars, median and IQR)				
GFAP immunohistochemistry in the corpus callosum of hydrocephalic rats (40× objective; scale bar, 10 µm). **a, c** Untreated hydrocephalic animals with moderate (**a**) and severe (**c**) hydrocephalus. **b, d** Dexamethasone-treated hydrocephalic animals with moderate (**b**) and severe (**d**) hydrocephalus				
GFAP and MBP concentrations by ELISA (ng/mL per µg total protein; logarithmic scale) in the cortex (**a, c**) and hippocampus (**b, d**). Individual animals; bars, median and IQR. Crosses indicate extreme values excluded from the primary analysis and retained in the sensitivity analysis				

Cortical MBP did not differ between HNT and C (ratio 0.89; 95% CI 0.55–1.46). It was lower in HTD than in HNT in the primary analysis (ratio 0.50; 95% CI 0.31–0.79; adjusted p = 0.026), but not after inclusion of one extreme HTD value (ratio 0.68; 95% CI 0.30–1.55) (Fig. 6c). Hippocampal MBP did not differ between groups (Fig. 6d).

Discussion

In young rats with kaolin-induced hydrocephalus, daily dexamethasone for 3 weeks did not improve ventricular size, spatial learning or memory, or biochemical markers of astroglial reactivity and myelin, and it caused marked growth restriction in hydrocephalic and non-hydrocephalic animals. Only a qualitative attenuation of callosal GFAP immunoreactivity and the absence of deaths among treated animals were positive factors.

Growth restriction was the most robust effect: treated hydrocephalic animals gained about one third of the weight gained by untreated ones. This agrees with the reduced body and brain weight, increased apoptosis and impaired learning seen after neonatal dexamethasone in rats, even at lower doses [3, 11,

16], with the weight loss reported in post-haemorrhagic hydrocephalus [24], and with adverse school-age outcomes after early postnatal dexamethasone in preterm infants [32]. The treatment window (PND 8–28) coincides with intense brain growth and myelination, and this toxicity plausibly offsets any anti-inflammatory benefit.

Likewise, dexamethasone did not improve water-maze performance. Interpretation is limited because untreated hydrocephalic animals did not differ from controls, so no deficit was present to be corrected. This may reflect the small HNT group and selective survival, as the five animals that died were presumably the most severely affected. Moreover, treated animals were much smaller, and swimming ability or general health may have influenced latencies independently of memory; the convergence of latencies by the last session suggests that they learned the task.

The astroglial findings were discordant. Attenuated callosal GFAP immunoreactivity agrees with reduced astrogliosis after dexamethasone in haemorrhagic hydrocephalus [24] and with other anti-inflammatory agents in the kaolin model [10, 13], but ELISA showed no reduction of hippocampal or cortical GFAP. Tissue GFAP content integrates astrocyte number and hypertrophy across a region and need not parallel staining in a single tract; without blinded quantification, the histological impression is preliminary. MBP was not reduced in untreated hydrocephalic animals, and the lower cortical MBP in treated animals was not robust; if confirmed, it would be consistent with dexamethasone-induced hypomyelination in the developing brain [3], in contrast with the improved myelination after a short tapering course in haemorrhagic hydrocephalus [24]. Dose, duration and the cause of hydrocephalus may determine the balance between benefit and toxicity.

The absence of mortality among treated animals is intriguing. Glucocorticoids reduce choroid plexus Na^+/K^+-ATPase activity and CSF formation [25, 30], and choroid plexus inflammation drives CSF hypersecretion [20]; either mechanism could limit acute decompensation, and a non-significant survival benefit was also observed by Lee et al. [24]. However, survival was not a pre-specified endpoint, causes of death were not established, ventricular ratios did not differ among survivors, and the higher proportion of treated animals without ventriculomegaly, although not significant, suggests that dexamethasone may have modified the response to kaolin. A dedicated study with survival as primary endpoint and serial imaging is warranted.

This study has several limitations. The hydrocephalic groups were small and unequal because of mortality and failure of induction, both of which may introduce selection bias, and the study was underpowered for moderate effects. A single dose and schedule were tested in male animals only. The randomization method, litter allocation and blinding of outcome assessment were not documented, and litter effects could not be modelled [23]. Effects of daily handling and injection cannot be separated from those of the drug. Immunohistochemistry was qualitative and limited to the corpus callosum, severity grades of hydrocephalus could not be reported, the water maze was not video-tracked, and the ELISA outlier rule was defined at the time of analysis; sensitivity analyses are therefore reported.

From a translational standpoint, broad glucocorticoid immunosuppression appears to be a poor strategy for neuroprotection in infantile hydrocephalus [6, 24]. Agents targeting specific pathways, such as cyclooxygenase-2 or microglial activation, may offer a better balance [10, 31]; if glucocorticoids are studied further, lower doses, shorter courses or less neurotoxic agents such as hydrocortisone [11] would be preferable.

Conclusion

In young rats with kaolin-induced hydrocephalus, dexamethasone (at 0.5 mg/kg/day for 21 days) caused marked growth restriction and did not improve ventricular size, spatial learning and memory, or changed the levels of biochemical markers of astrogliosis and myelin. These data do not support dexamethasone at this regimen as a neuroprotective adjunct to the surgical treatment of hydrocephalus in the developing brain.

Declarations

Competing interests

The authors have no relevant financial or non-financial interests to disclose.

Ethics approval

All procedures were approved by the Ethics Committee on Animal Use of the Ribeirão Preto Medical School, University of São Paulo (CEUA-FMRP-USP) and followed the guidelines of the Brazilian College of Animal Experimentation (COBEA).

Consent to participate/ for publication Not applicable.

Funding

This work was supported by the Programa Unificado de Bolsas de Estudo para Apoio à Formação de Estudantes de Graduação (PUB), University of São Paulo (scholarship to Larissa Caires Giglio, 2023–2024).

Author Contribution

All authors conceived and designed the study. Larissa Caires Giglio performed the experiments and collected the data. Luiza da Silva Lopes was responsible for the animal-ethics reporting and project administration. Otávio da Cunha Ferreira Neto and Matheus Nagai Ribeiro do Val performed the statistical re-analysis and revised the manuscript. Marcelo Volpon Santos, Hélio Rubens Machado and

Luiza da Silva Lopes supervised the study. All authors contributed to data acquisition or interpretation, critically revised the manuscript, and read and approved the final version.

References

1. Bothwell SW, Janigro D, Patabendige A (2019) Cerebrospinal fluid dynamics and intracranial pressure elevation in neurological diseases. Fluids Barriers CNS 16(1):9. 10.1186/s12987-019-0129-6
2. Brouwer MC, Heckenberg SG, de Gans J et al (2010) Nationwide implementation of adjunctive dexamethasone therapy for pneumococcal meningitis. Neurology 75(17):1533–1539. 10.1212/WNL.0b013e3181f96297
3. Chang YP (2014) Evidence for adverse effect of perinatal glucocorticoid use on the developing brain. Korean J Pediatr 57(3):101–109. 10.3345/kjp.2014.57.3.101
4. Cruz-Topete D, Cidlowski JA (2015) One hormone, two actions: anti- and pro-inflammatory effects of glucocorticoids. Neuroimmunomodulation 22(1–2):20–32. 10.1159/000362724
5. de Moura Silva GAP, da Silva SC, da Silva Beggiora P et al (2021) Transcranial ultrasonography as a reliable instrument for the measurement of the cerebral ventricles in rats with experimental hydrocephalus: a pilot study. Childs Nerv Syst 37(6):1863–1869. 10.1007/s00381-021-05070-6
6. Del Bigio MR, Di Curzio DL (2016) Nonsurgical therapy for hydrocephalus: a comprehensive and critical review. Fluids Barriers CNS 13:3. 10.1186/s12987-016-0025-2
7. Del Bigio MR (2010) Neuropathology and structural changes in hydrocephalus. Dev Disabil Res Rev 16(1):16–22. 10.1002/ddrr.94
8. Del Bigio MR (2001) Pathophysiologic consequences of hydrocephalus. Neurosurg Clin N Am 12(4):639–649
9. Deren KE, Packer M, Forsyth J et al (2010) Reactive astrocytosis, microgliosis and inflammation in rats with neonatal hydrocephalus. Exp Neurol 226(1):110–119. 10.1016/j.expneurol.2010.08.010
10. Dutra M, Covas da Silva S, da Silva Beggiora Marques P et al (2023) Celecoxib attenuates neuroinflammation, reactive astrogliosis and promotes neuroprotection in young rats with experimental hydrocephalus. J Chem Neuroanat 133:102344. 10.1016/j.jchemneu.2023.102344
11. Feng Y, Kumar P, Wang J, Bhatt AJ (2015) Dexamethasone but not the equivalent doses of hydrocortisone induces neurotoxicity in neonatal rat brain. Pediatr Res 77(5):618–624. 10.1038/pr.2015.19
12. Fietta P, Fietta P, Delsante G (2009) Central nervous system effects of natural and synthetic glucocorticoids. Psychiatry Clin Neurosci 63(5):613–622. 10.1111/j.1440-1819.2009.02005.x
13. Garcia CAB, Catalão CHR, Machado HR et al (2017) Edaravone reduces astrogliosis and apoptosis in young rats with kaolin-induced hydrocephalus. Childs Nerv Syst 33(3):419–428. 10.1007/s00381-016-3313-x

14. Garne E, Loane M, Addor MC et al (2010) Congenital hydrocephalus–prevalence, prenatal diagnosis and outcome of pregnancy in four European regions. Eur J Paediatr Neurol 14(2):150–155. 10.1016/j.ejpn.2009.03.005
15. Gundamraj S, Hasbun R (2020) The use of adjunctive steroids in central nervous infections. Front Cell Infect Microbiol 10:592017. 10.3389/fcimb.2020.592017
16. Ichinohashi Y, Sato Y, Saito A et al (2013) Dexamethasone administration to the neonatal rat results in neurological dysfunction at the juvenile stage even at low doses. Early Hum Dev 89(5):283–288. 10.1016/j.earlhumdev.2012.10.007
17. Jeng S, Gupta N, Wrensch M et al (2011) Prevalence of congenital hydrocephalus in California, 1991–2000. Pediatr Neurol 45(2):67–71. 10.1016/j.pediatrneurol.2011.03.009
18. Jucá CEB, Lins Neto A, Oliveira RS, Machado HR (2002) Tratamento de hidrocefalia com derivação ventrículo-peritoneal: análise de 150 casos consecutivos no Hospital das Clínicas de Ribeirão Preto. Acta Cir Bras 17:59–63
19. Kahle KT, Kulkarni AV, Limbrick DD Jr, Warf BC (2016) Hydrocephalus in children. Lancet 387(10020):788–799. 10.1016/S0140-6736(15)60694-8
20. Karimy JK, Zhang J, Kurland DB et al (2017) Inflammation-dependent cerebrospinal fluid hypersecretion by the choroid plexus epithelium in posthemorrhagic hydrocephalus. Nat Med 23(8):997–1003. 10.1038/nm.4361
21. Khan OH, Enno TL, Del Bigio MR (2006) Brain damage in neonatal rats following kaolin induction of hydrocephalus. Exp Neurol 200(2):311–320. 10.1016/j.expneurol.2006.02.113
22. Kurt G, Cemil B, Borcek AO et al (2010) Infliximab administration reduces neuronal apoptosis on the optic pathways in a rabbit hydrocephalus model: a preliminary report. Br J Neurosurg 24(3):275–279. 10.3109/02688691003653751
23. Lazic SE, Essioux L (2013) Improving basic and translational science by accounting for litter-to-litter variation in animal models. BMC Neurosci 14:37. 10.1186/1471-2202-14-37
24. Lee JH, Chang YS, Ahn SY, Sung SI, Park WS (2018) Dexamethasone does not prevent hydrocephalus after severe intraventricular hemorrhage in newborn rats. PLoS ONE 13(10):e0206306. 10.1371/journal.pone.0206306
25. Lindvall-Axelsson M, Hedner P, Owman C (1989) Corticosteroid action on choroid plexus: reduction in Na+-K+-ATPase activity, choline transport capacity, and rate of CSF formation. Exp Brain Res 77(3):605–610. 10.1007/BF00249613
26. McAllister JP 2nd, Miller JM (2010) Minocycline inhibits glial proliferation in the H-Tx rat model of congenital hydrocephalus. Cerebrospinal Fluid Res 7:7. 10.1186/1743-8454-7-7
27. Percie du Sert N, Hurst V, Ahluwalia A et al (2020) The ARRIVE guidelines 2.0: updated guidelines for reporting animal research. PLoS Biol 18(7):e3000410. 10.1371/journal.pbio.3000410
28. Rekate HL (2008) The definition and classification of hydrocephalus: a personal recommendation to stimulate debate. Cerebrospinal Fluid Res 5:2. 10.1186/1743-8454-5-2

29. Vorhees CV, Williams MT (2006) Morris water maze: procedures for assessing spatial and related forms of learning and memory. Nat Protoc 1(2):848–858. 10.1038/nprot.2006.116
30. Weiss MH, Nulsen FE (1970) The effect of glucocorticoids on CSF flow in dogs. J Neurosurg 32(4):452–458. 10.3171/jns.1970.32.4.0452
31. Xu H, Tan G, Zhang S et al (2012) Minocycline reduces reactive gliosis in the rat model of hydrocephalus. BMC Neurosci 13:148. 10.1186/1471-2202-13-148
32. Yeh TF, Lin YJ, Lin HC et al (2004) Outcomes at school age after postnatal dexamethasone therapy for lung disease of prematurity. N Engl J Med 350(13):1304–1313. 10.1056/NEJMoa032089

Figures

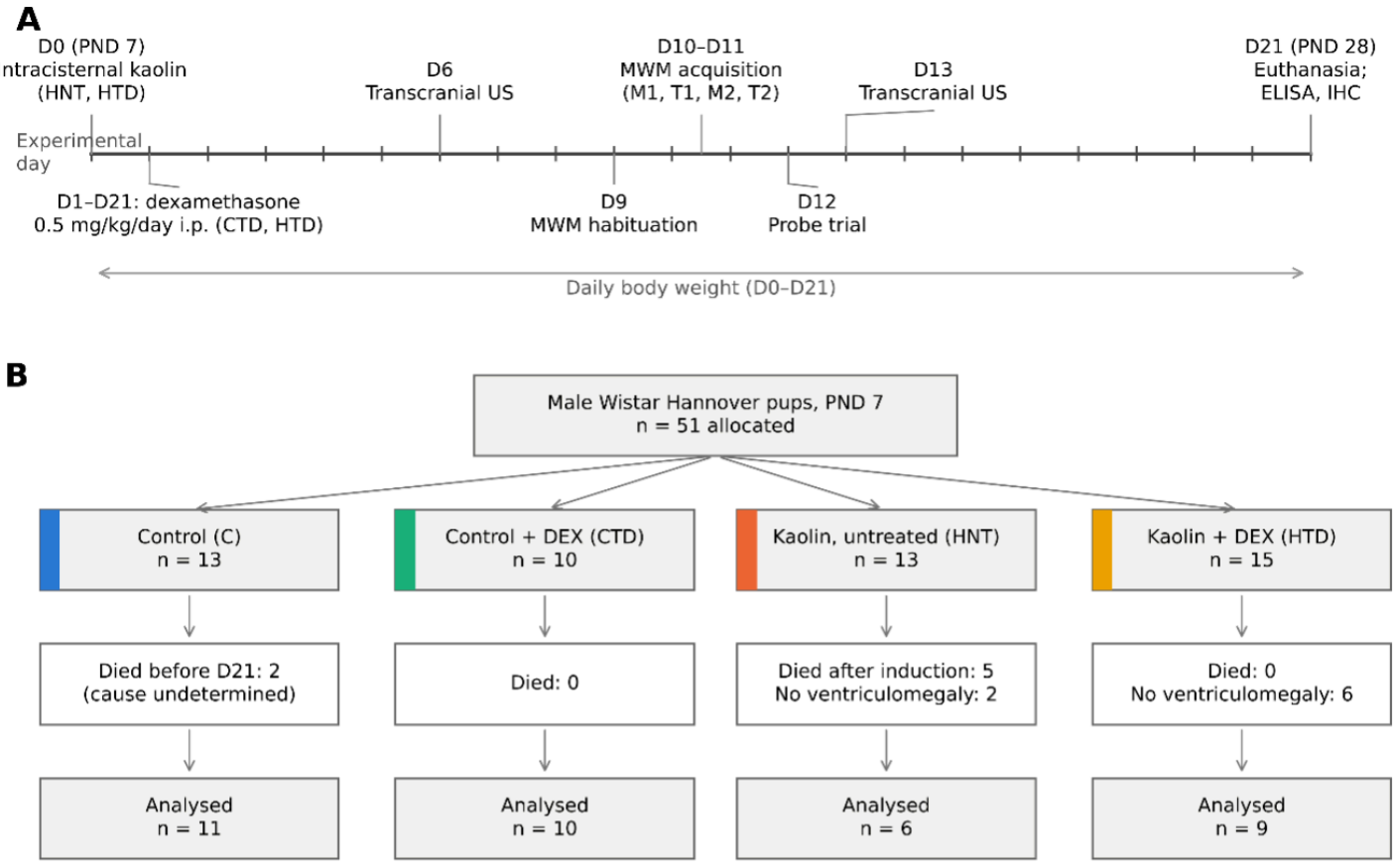


Figure 1

Study design. **a** Experimental timeline; experimental day 0 (D0) corresponds to postnatal day (PND) 7. US, transcranial ultrasonography; MWM, Morris water maze; IHC, immunohistochemistry. **b**Flow of animals through the study. C, control; CTD, dexamethasone-treated control; HNT, untreated hydrocephalic; HTD, dexamethasone-treated hydrocephalic

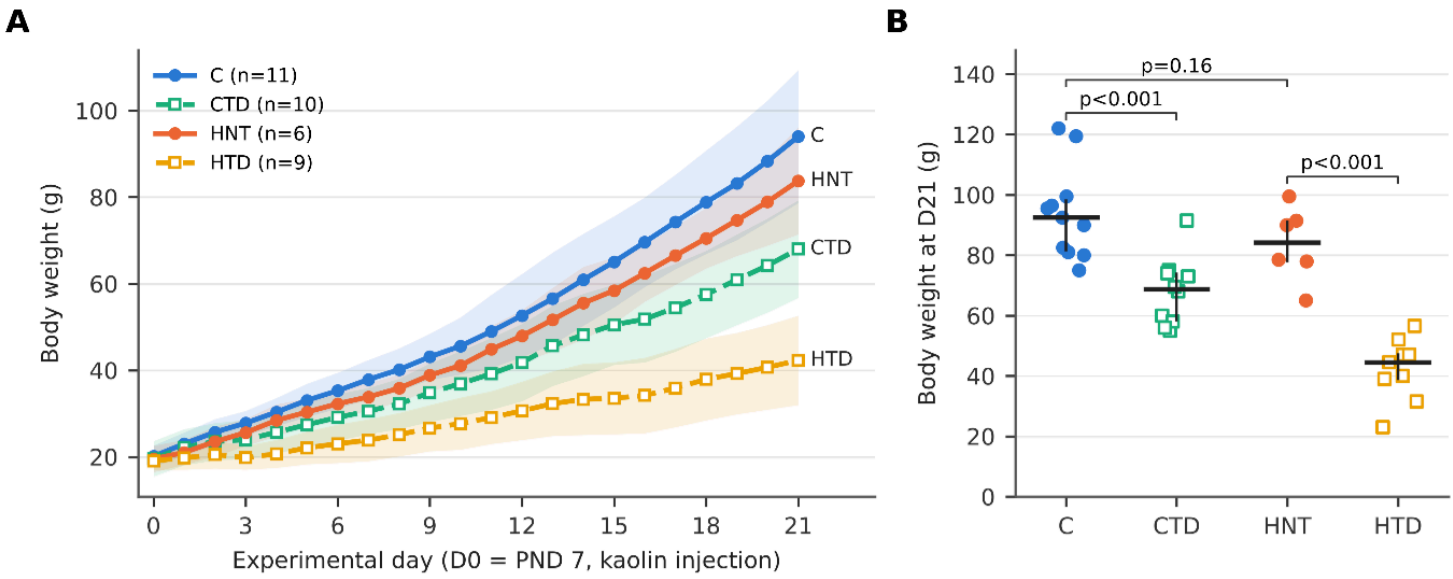


Figure 2

Body weight. **a** Daily body weight from D0 to D21 (mean ± SD, shaded). **b** Body weight on D21 in individual animals (bars, median and interquartile range); p-values are Holm-adjusted Welch contrasts. Filled symbols, untreated; open symbols, dexamethasone

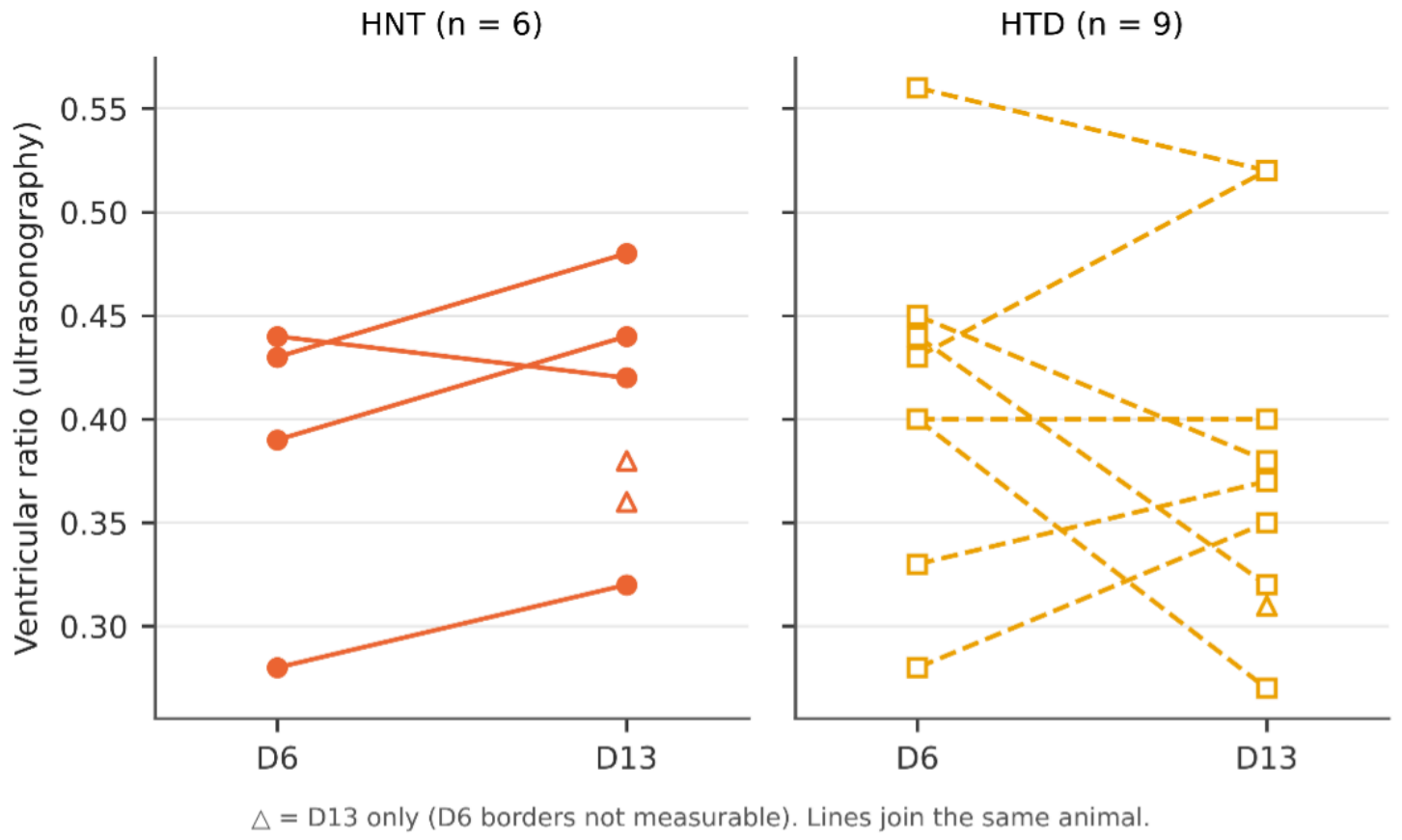


Figure 3

Ventricular ratio on transcranial ultrasonography on D6 and D13 in untreated (HNT) and dexamethasone-treated (HTD) hydrocephalic rats. Lines join measurements from the same animal; triangles indicate animals whose ventricular borders could not be identified on D6

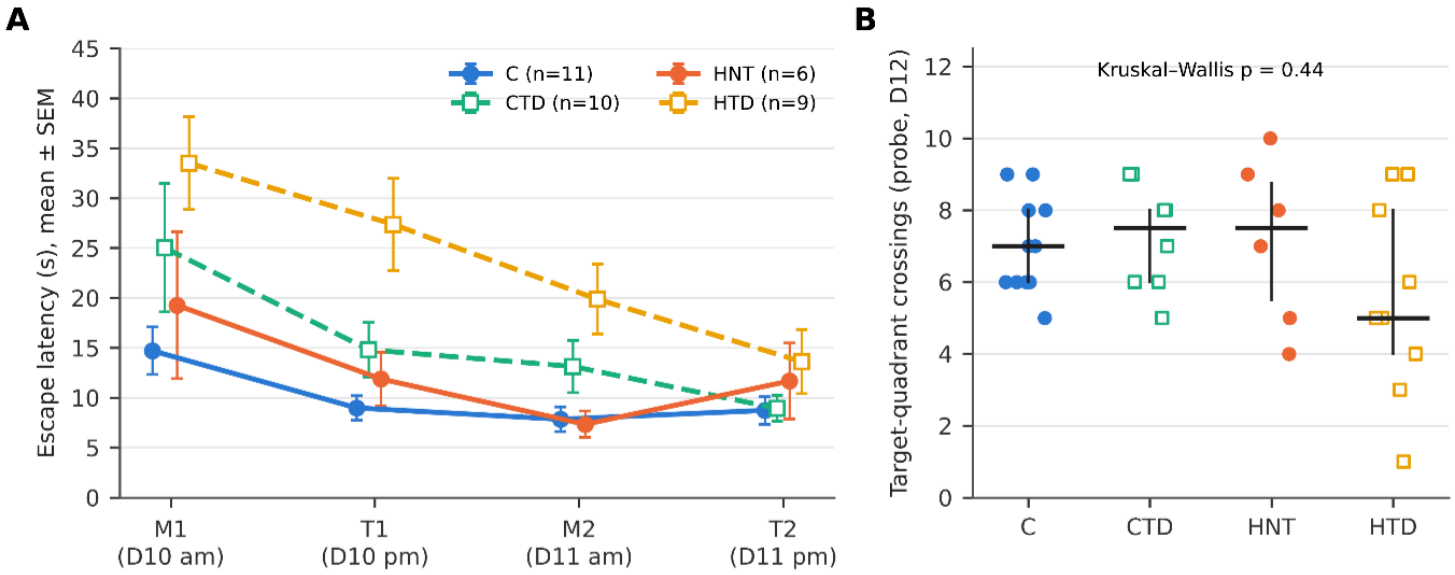


Figure 4

Morris water maze. **a** Escape latency in the four acquisition sessions (mean ± SEM); M1/T1, morning/afternoon of D10; M2/T2, morning/afternoon of D11. **b** Crossings of the former platform quadrant in the probe trial on D12 (individual animals; bars, median and IQR)

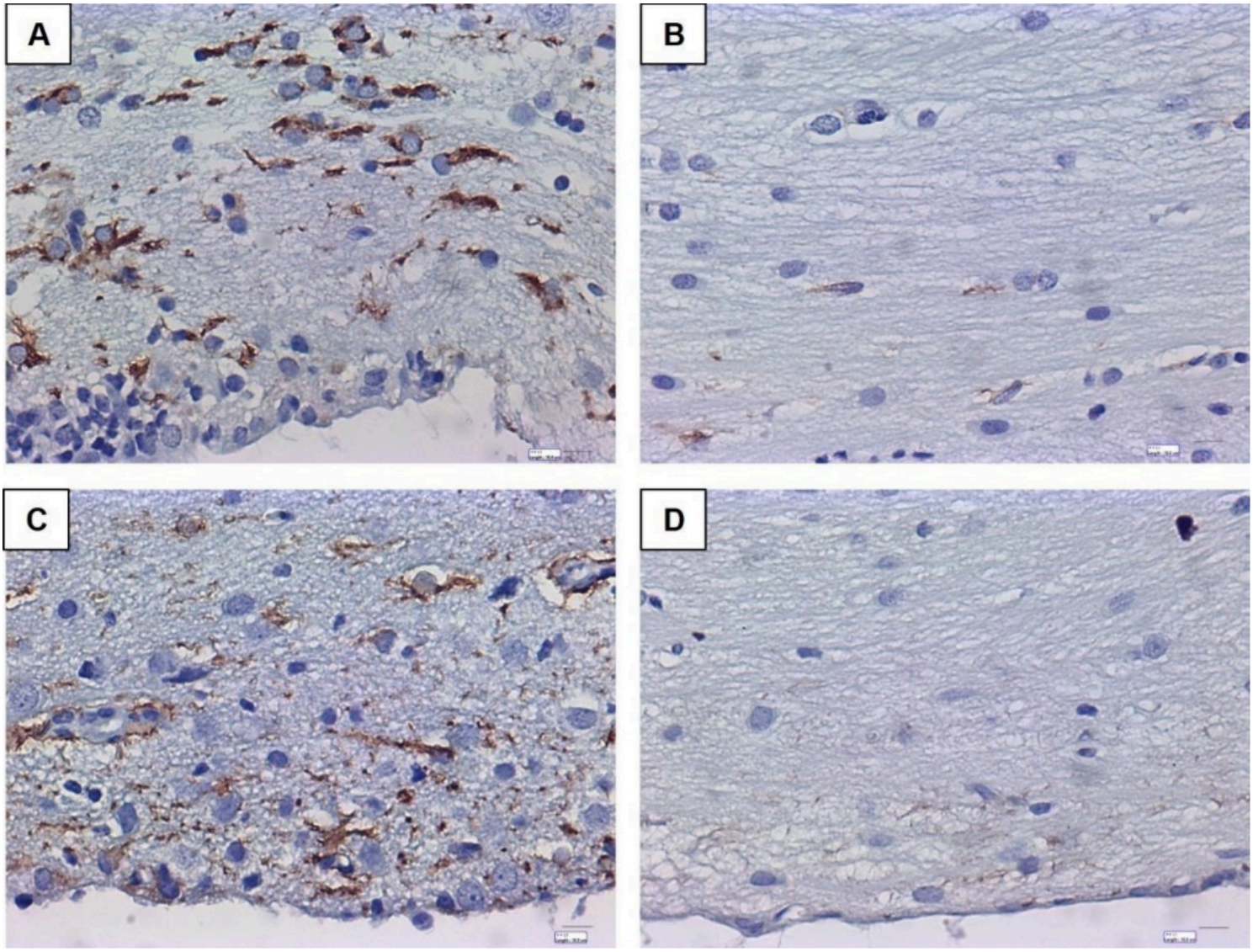


Figure 5

GFAP immunohistochemistry in the corpus callosum of hydrocephalic rats (40× objective; scale bar, 10 μm). **a, c**Untreated hydrocephalic animals with moderate (**a**) and severe (**c**) hydrocephalus. **b, d** Dexamethasone-treated hydrocephalic animals with moderate (**b**) and severe (**d**) hydrocephalus

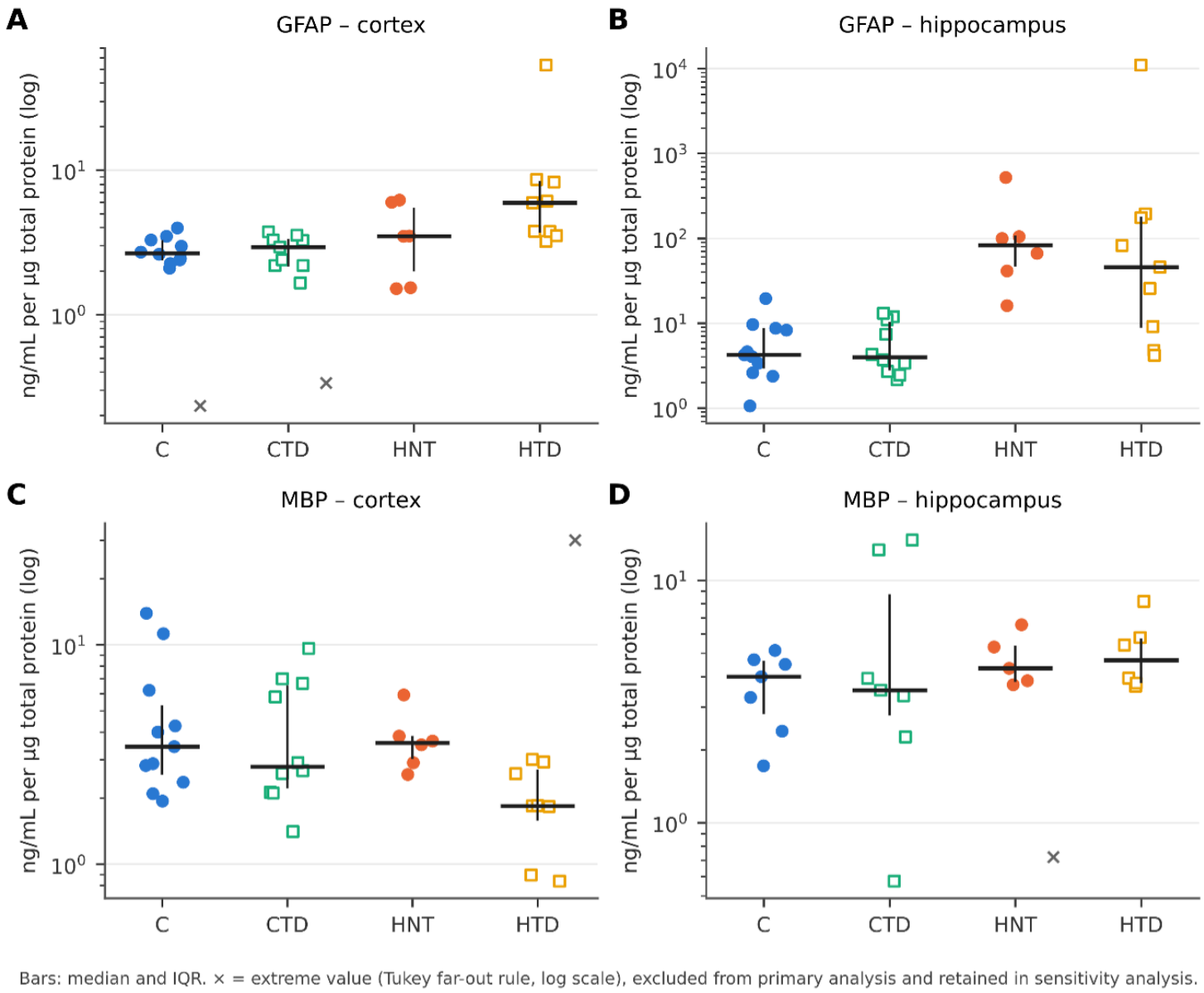


Figure 6

GFAP and MBP concentrations by ELISA (ng/mL per µg total protein; logarithmic scale) in the cortex (**a, c**) and hippocampus (**b, d**). Individual animals; bars, median and IQR. Crosses indicate extreme values excluded from the primary analysis and retained in the sensitivity analysis